



Scholars Research Library
(<http://scholarsresearchlibrary.com/archive.html>)



ISSN : 2231- 3176
CODEN (USA): JCMMDA

Exploration of the mechanism and selectivity of [1+2] cycloaddition reaction between α -cis-himachalene and dibromocarbene using DFT-based reactivity indices

Redouan Hammal¹, Ahmed Benharref² and Abdeslam El Hajbi^{1*}

¹Physical Chemistry Laboratory, Chemistry Department, Faculty of Science, Chouaïb Doukkali University, El Jadida, Morocco

²Laboratory of Biomolecular Chemistry, Natural Substances and Reactivity (URAC 16), Cadi Ayyad University, Semlalia Faculty of Science, Marrakech, Morocco

ABSTRACT

In this work we used DFT B3LYP/6-311+G** to study the mechanism and the regio- and stereoselectivity of the [1+2] cycloaddition reaction between α -cis-himachalene and dibromocarbene. We found that the reaction follows a concerted asynchronous mechanism and is exothermic and stereoselective. Treatment of α -cis-himachalene with one equivalent of dibromocarbene leads to the formation of two products resulting from attack of the most substituted double bond of α -cis-himachalene. Treatment of α -cis-himachalene with two equivalents of dibromocarbene leads to formation of two products resulting from attack of the exocyclic double bond.

Key words: Frontier molecular orbital theory, electrophilicity, nucleophilicity, reactivity index, transition state theory.

INTRODUCTION

This work follows on from our study of the reactivity of the essential oil of the Atlas Cedar, *Cedrus atlantica*, which is used in perfumery and cosmetics [1]. A number of studies have investigated the isolation and identification of this oil, and the reactivity of its constituents [2-6].

The essential oil of the Atlas Cedar is principally composed (75%) of three bicyclic sesquiterpenic hydrocarbons, namely α -cis-himachalene, β -himachalene and γ -cis-himachalene. When these are treated with hydrochloric acid in acetic acid, followed by dehydrogenation in a basic environment, α -trans-himachalene is formed [7-9]. The reactivity of these sesquiterpenes has been studied [4, 10-12]. Studies have also been carried out on the reactivity of the himachalenes (hemisynthesis) in order to obtain new compounds with olfactory properties of interest to the perfume industry [13-15]. In our study we looked at the action of two different quantities of dibromocarbene on α -cis-himachalene, and analysed the chemo-, regio- and stereoselectivity of these reactions. A stoichiometric quantity of dibromocarbene led to attack at α side of the most substituted double bond, while an excess of dibromocarbene led to attack at the exocyclic double bond of α -cis-himachalene. This shows that the endocyclic double bond of the α -cis- and α -trans-himachalene behaves in the same way, while the exocyclic double bond behaves differently in the two compounds [1].

By carrying out theoretical calculations regarding the behaviour of α -cis-himachalene in the presence of dibromocarbene we have been able to predict chemoselectivity using frontier orbital theory, and to analyse regio- and stereoselectivity using reactivity indices and activation energies of the transition states. Experiments have shown

that the action of a stoichiometric quantity of dibromocarbene on α -cis-himachalene produces a majority of the α regioisomer, referred to here as $P_1(\alpha)$, and a minority of the β regioisomer, referred to as $P_1(\beta)$. Reaction between α -cis-himachalene and an excess of dibromocarbene leads to the formation of a majority of the α regioisomer, referred to as $P_2(\alpha)$, and a minority of the β regioisomer, referred to as $P_2(\beta)$ (Figure 1).

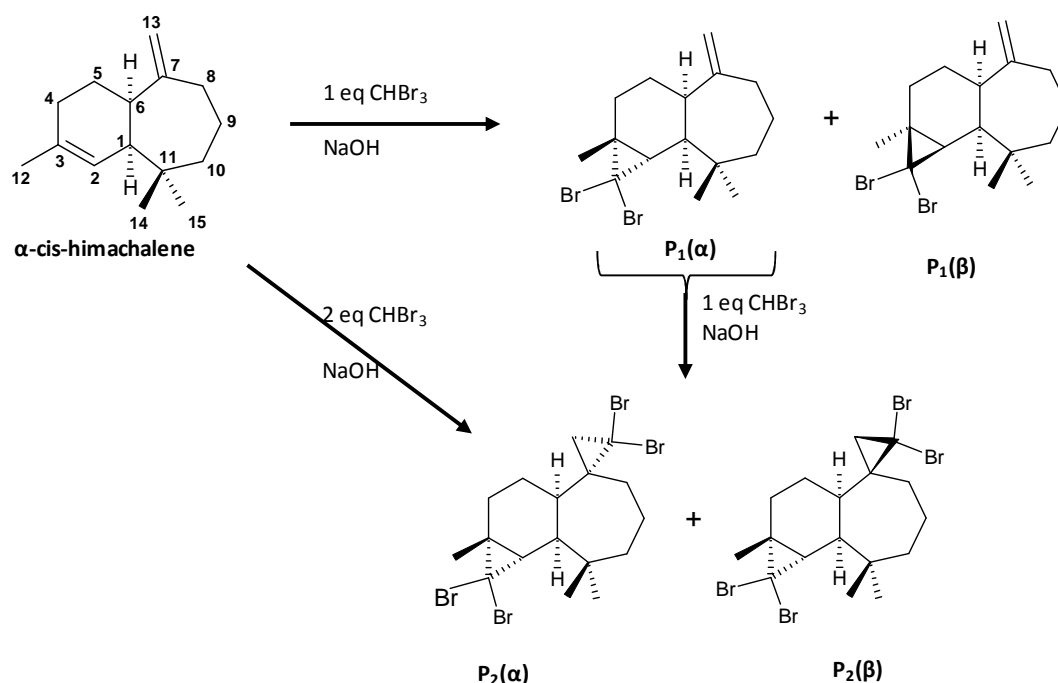


Figure 1. Reaction between dibromocarbene and α -cis-himachalene

MATERIALS AND METHODS

We used DFT B3LYP/6-311+G** to study the mechanism and equilibrium geometries of the reaction between α -cis-himachalene and dibromocarbene, together with the transition states corresponding to the two approaches at the α and β sides [16-17]. We identified the transition states and confirmed their existence by the presence of a single imaginary frequency in the Hessian matrix. We calculated and plotted the intrinsic reaction coordinate (IRC) [18] in order to show that the transition state is indeed linked to the two minima (reactants and product). We analysed the electronic structures of the stationary points and the bond orders (Wiberg indices) [19] using the natural bond orbital method (NBO) [20-21]. We calculated the values of enthalpies, entropies and free energies using standard statistical thermodynamics. All calculations were carried out using the DFT B3LYP/6-311+G** method in Gaussian 09 [22].

In order to demonstrate the nucleophilic/electrophilic nature of the reactants, we calculated the electronic chemical potential μ and the global hardness η . These two values can be calculated from the energies of the HOMO and LUMO frontier molecular orbitals, with $\mu=(E_{\text{HOMO}}+E_{\text{LUMO}})/2$ and $\eta=(E_{\text{LUMO}}-E_{\text{HOMO}})$ [23]. The global electrophilicity index $\omega=(\mu^2/2\eta)$ [24] is also defined as the energy stabilisation due to charge transfer [25]. The nucleophilicity index N is expressed as a function of the HOMO energy of tetracyanoethylene (TCNE) as $N=E_{\text{HOMO}}(\text{Nu})-E_{\text{HOMO}}(\text{TCE})$ [26].

Reactivity indices were calculated from the HOMO and LUMO energies in the fundamental state of the molecules using DFT B3LYP/6-311+G**. The static local electrophilicity and nucleophilicity indices are reliable predictors of the most favoured electrophile-nucleophile interaction for the formation of a chemical bond between two atoms [25, 27]. The expressions $\omega_k=\omega \cdot P_{k+}$ and $N_k=N \cdot P_{k-}$ correspond respectively to the local electrophilicity index ω_k and the local nucleophilicity index N_k . P_{k+} and P_{k-} are obtained by analysing the Mulliken spin density of the anion and the cation [28].

1. Analysis of results

1.1. Analysis of the reactivity indices of the reactants in the fundamental state

1.1.1. Predicting the Normal Electron Demand (NED) / Inverse Electron Demand (IED) characteristics of the reaction

We used frontier molecular orbital theory to predict whether the reaction between α -cis-himachalene and dibromocarbene can be characterised as NED (Normal Electron Demand) or IED (Inverse Electron Demand). Global and local indices as defined by conceptual DFT are effective tools for studying the reactivity of polar interactions [29].

Chemical electron potential μ , chemical hardness η , global electrophilicity ω and global nucleophilicity N are global properties of α -cis-himachalene and dibromocarbene which allow us to analyse the reactivity at various sites on these reactants. The energy gap between the HOMO of α -cis-himachalene and the LUMO of dibromocarbene is 2.4966 eV, while the energy gap between the HOMO of dibromocarbene and the LUMO of α -cis-himachalene is 7.4233 eV (Table 1). This shows that α -cis-himachalene behaves as a nucleophile, while dibromocarbene is an electrophile. The localisation of the HOMO and LUMO of α -cis-himachalene and dibromocarbene are shown in Figure 2.

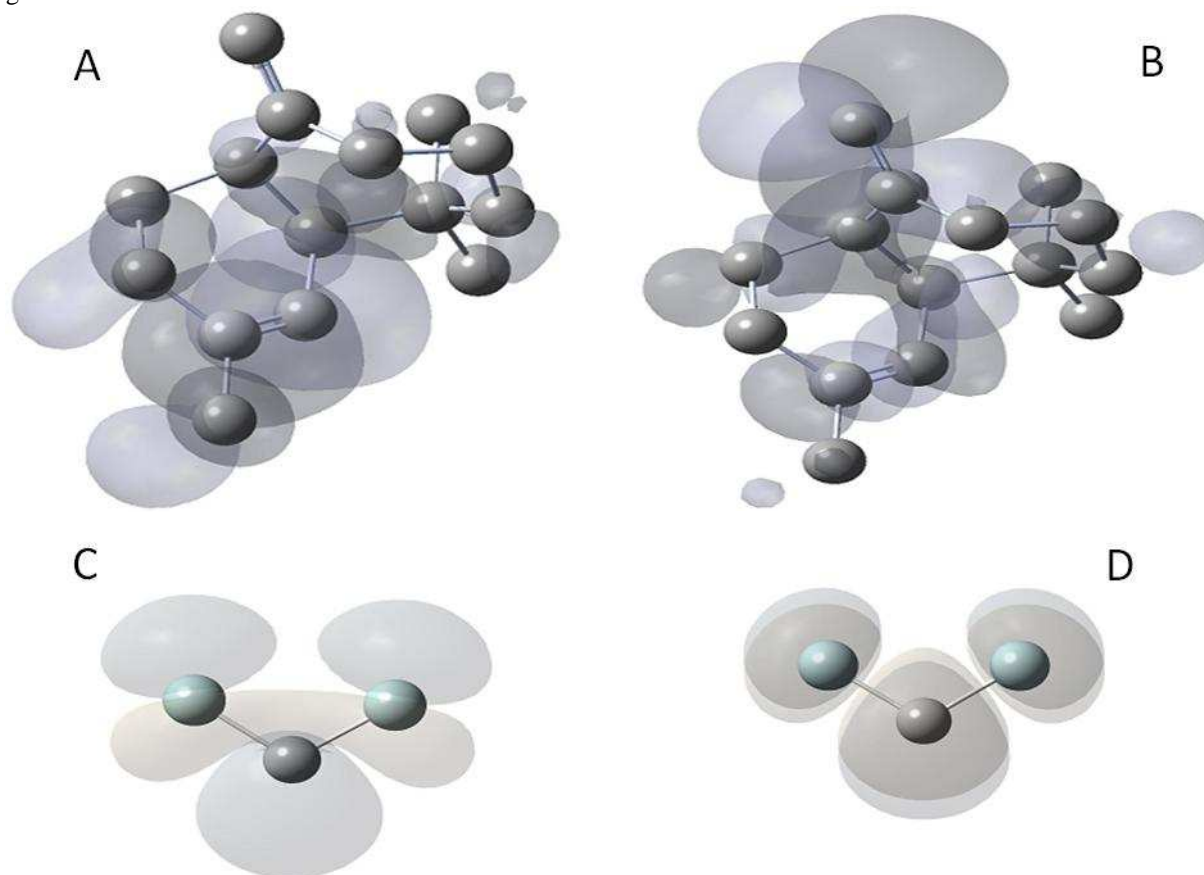


Figure 2. Isodensity map of the HOMO and LUMO of α -cis-himachalene and dibromocarbene
 α -cis-himachalene A. HOMO B. LUMO
 Dibromocarbene C. HOMO D. LUMO

Table 1. Energy gap between HOMO and LUMO in the reaction between α -cis-himachalene and dibromocarbene

	HOMO	LUMO	E_{HOMO} (α -cis-himachalene) - E_{LUMO} (dibromocarbene)	E_{LUMO} (dibromocarbene) - E_{HOMO} (α -cis-himachalene)
α -cis-himachalene	-6.3269	0.2057	2.4966	7.4233
Dibromo-carbene	-7.2176	-3.8303		

Table 2 shows that the electronic chemical potential μ of α -cis-himachalene is greater than that of dibromocarbene, while the global electrophilicity index ω of dibromocarbene is greater than that of α -cis-himachalene. These results confirm that α -cis-himachalene is a nucleophile and that dibromocarbene is an electrophile, which implies that

charge transfer takes place from α -cis-himachalene to dibromocarbene. The significant difference in electrophilicity ($\Delta\omega = 3.7872$ eV) between α -cis-himachalene and dibromocarbene shows a high NED polarity for this reaction.

Table 2. Electronic chemical potential μ , hardness η , global electrophilicity ω and global nucleophilicity N of α -cis-himachalene and dibromocarbene (eV)

	μ	η	ω	N
α -cis-himachalene	-3.0606	6.5326	0.7170	3.0417
Dibromocarbene	-5.5239	3.3873	4.5042	2.1511

1.1.2. Using electrophilicity and nucleophilicity indices to predict the regio- and stereoselectivity of the reaction

According to the polar model proposed by Chattaraj [30] the local philicity indices (ω_k and N_k) are reliable indicators for predicting the most favoured interaction between two polar centres. The most favoured regioisomer is that which is associated with the highest local electrophilicity index ω_k of the electrophile and the highest local nucleophilicity index N_k of the nucleophile. We determined N_k for α -cis-himachalene and ω_k for dibromocarbene in order to predict the most likely electrophile/nucleophile interaction throughout the reaction pathway, in order to elucidate the chemo- and stereoselectivity of the reaction. The C carbon of dibromocarbene is the most electrophilic active site ($\omega_C=4.4106$ eV). The C₂ and C₃ carbon atoms of the endocyclic double bond of α -cis-himachalene are more strongly nucleophilic and more active than those of the C₇ and C₁₃ atoms of the exocyclic double bond. Furthermore, the C₂ carbon atom is the most nucleophilic site of α -cis-himachalene ($N_{C_2}=0.9255$ eV). Figure 3 shows the most active sites of α -cis-himachalene and dibromocarbene. We can deduce that the most favoured interaction will take place between the C₂ atom of α -cis-himachalene and the carbon atom of dibromocarbene, followed by closure of the cycle with the formation of the second C-C₃ bond. The interaction between the nucleophile α -cis-himachalene and the electrophile dibromocarbene is therefore competitive.

The majority products obtained from this reaction are indeed linked to the two active C=C sites of α -cis-himachalene. Figure 4 shows that the attack leads to the formation of two chemoisomers, each of which consists of two regioisomers α and β .

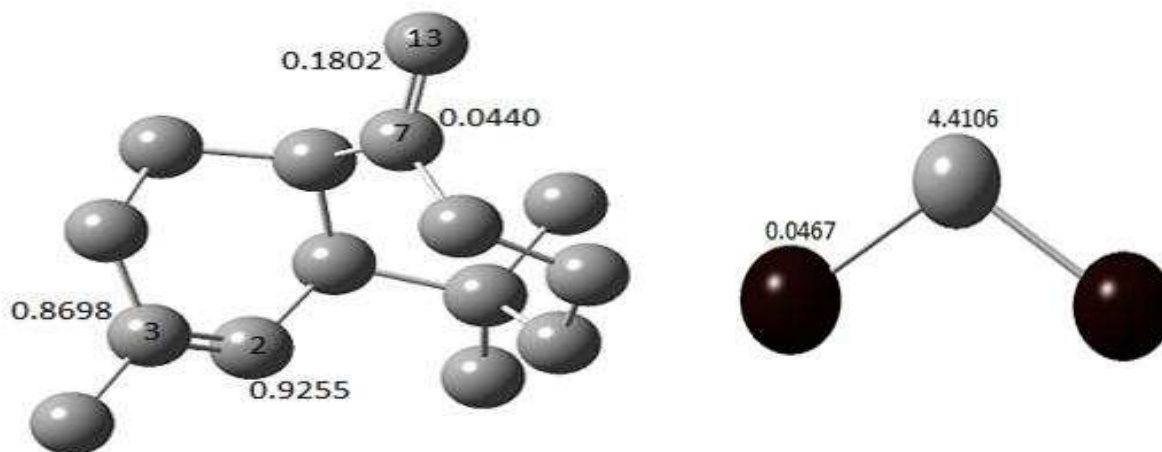


Figure 3. Local nucleophilicity (N_k) of α -cis-himachalene and local electrophilicity (ω_k) of dibromocarbene (eV)

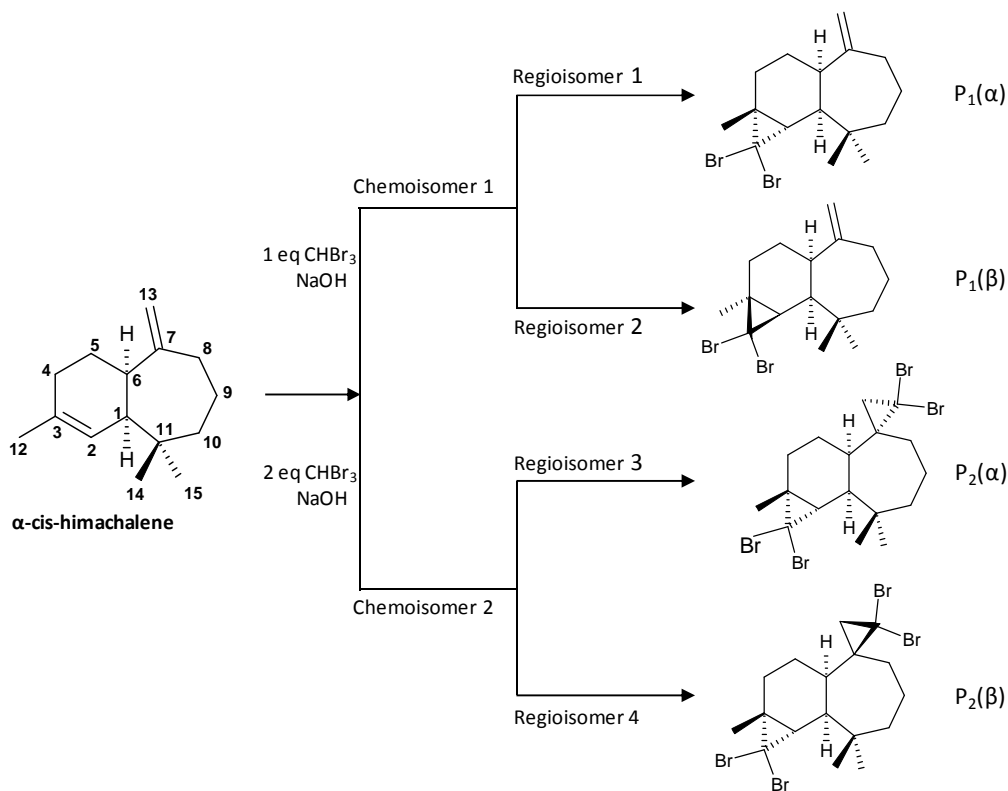


Figure 4. Reaction between α -cis-himachalene and dibromocarbene showing chemoselectivity

1.2. Study of the mechanism of the reaction between α -cis-himachalene and dibromocarbene

1.2.1. Analysis of the potential energy surface and prediction of the reaction mechanism

Figure 5 shows the transition states corresponding to the two chemoisomers in the reaction between α -cis-himachalene and dibromocarbene (stoichiometric reaction followed by reaction with an excess of dibromocarbene). The activation energy of transition state TS_1 (corresponding to the α side) is 4.5944 kcal/mol, i.e. 10.4592 kcal/mol below TS_2 (corresponding to the β side) showing that the α regioisomer is kinetically preferred to the β regioisomer in the stoichiometric reaction. An excess of dibromocarbene results in two transition states: TS_3 (corresponding to the α side) with an activation energy of 3.9529 kcal/mol, i.e. 2.5829 kcal/mol below TS_4 (corresponding to the β side), indicating that the regioisomer corresponding to the α side is kinetically preferred to the β regioisomer.

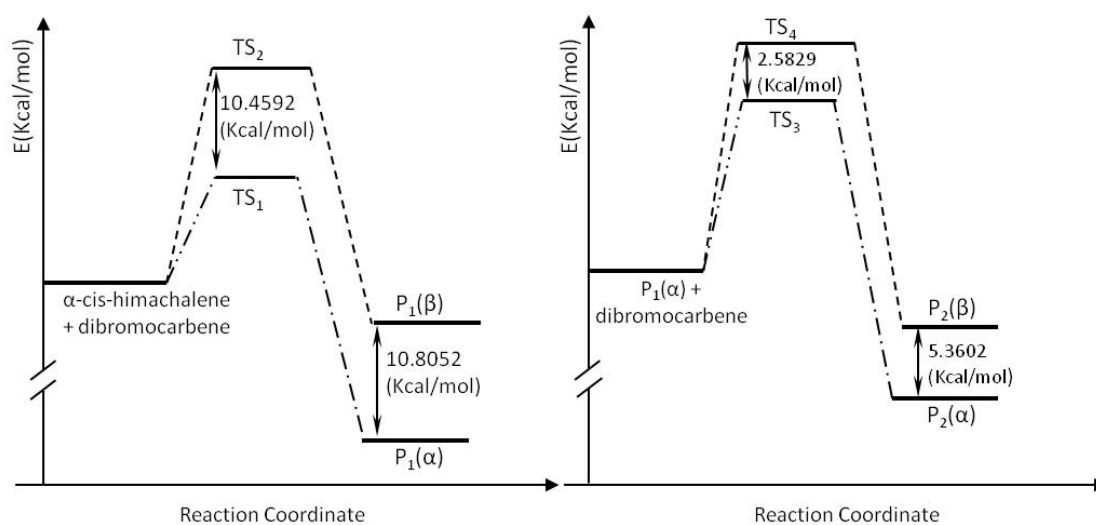


Figure 5. Energy profile of the reaction between α -cis-himachalene and dibromocarbene showing chemoselectivity (kcal/mol)

1.2.2. Analysis of the IRC of the reaction between α -cis-himachalene and dibromocarbene

The cycloaddition reaction may have one of two main mechanisms, concerted or stepwise. The concerted mechanism involves a single step with asynchronous formation of two bonds, or a single step with two phases, characterised by the formation of the first bond σ followed by closure of the cycle without the formation of a stable intermediary reactant, while the two-step mechanism involves an intermediary reactant. We studied the molecular system as it develops during the reaction between α -cis-himachalene and dibromocarbene by calculating the intrinsic reaction coordinate (IRC) in order to show that the transition state is indeed linked to the two minima (reactants and product).

The plots $E=f(\text{RC})$ corresponding to all possible pathways are shown in Figure 6. IRC calculation shows that this reaction follows a concerted mechanism in a single step but in two phases[31] chemoisomer 1 corresponds to the formation of the C-C₂ bond, followed by closure of the cycle with the C-C₃ bond, while chemoisomer 2 corresponds to the formation of the C-C₁₃ bond, followed by closure of the cycle with the C-C₇ bond. Analysis of the IRC calculated using DFT B3LYP/6-311+G** shows that whatever quantity of dibromocarbene is used in the interaction with α -cis-himachalene, the transition states are reached without going through a stable intermediary stage.

Tables 3 and 4 show that after making thermal corrections for the thermodynamic energies, the free activation enthalpies of TS₁ and TS₂ increase by 17.9649 kcal/mol and 28.4055 kcal/mol respectively, while the free activation enthalpies of TS₃ and TS₄ increase by 16.7727 kcal/mol and 20.1229 kcal/mol respectively. These high values are a result of the unfavourable activation entropies associated with the process.

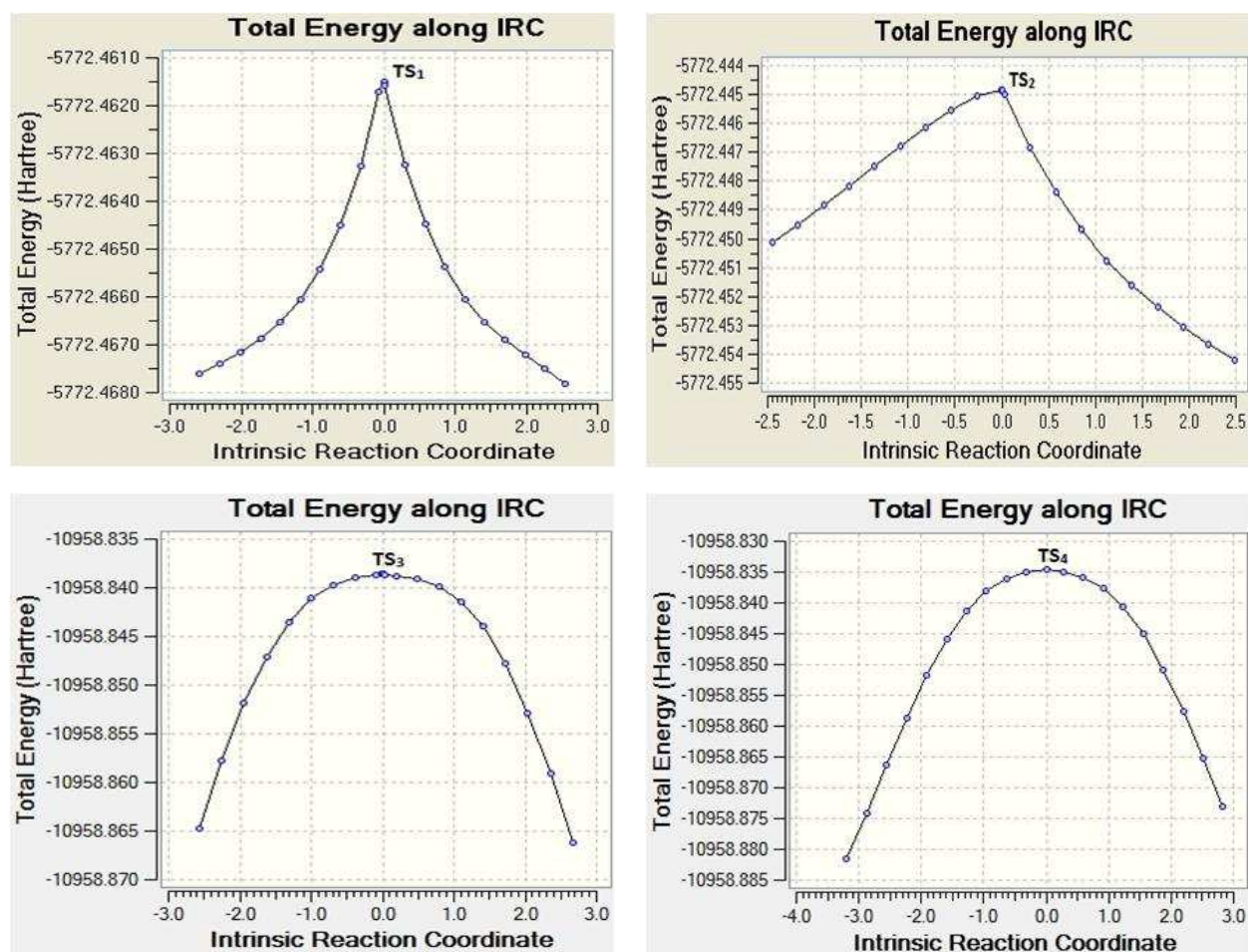


Figure 6. IRC of the reaction between α -cis-himachalene and dibromocarbene calculated using B3LYP/6-311+G**

The products P₁(α) and P₁(β) obtained for a stoichiometric quantity of the reactants are strongly exothermic, by -52.7162 kcal/mol and -41.9110 kcal/mol respectively. Consequently, P₁(α) is thermodynamically preferred to P₁(β). In the second reaction (excess of dibromocarbene), products P₂(α) and P₂(β) are also exothermic, by -54.7898 kcal/mol and -49.4216 kcal/mol respectively, indicating that P₂(α) is thermodynamically preferred to P₂(β).

Table 3. Thermodynamic energies of the reaction between α -cis-himachalene and one equivalent of dibromocarbene calculated using DFT B3LYP/6-311+G**

	α -cis-himachalene	Dibromo-carbene	TS ₁	TS ₂	P ₁ (α)	P ₁ (β)
<i>E</i> (au)	-586.1767	-5186.2921	-5772.4615	-5772.4448	-5772.5528	-5772.5356
ΔE (Kcal/mol)			4.5944	15.0536	-52.7162	-41.9110
<i>H</i> (au)	-585.8050	-5186.2843	-5772.0806	-5772.0637	-5772.1680	-5772.1507
ΔH (Kcal/mol)			5.4644	16.0304	-49.4139	-38.5573
<i>S</i> (cal/mol.K)	117.6810	69.0900	144.8440	145.2640	138.5690	137.9350
ΔS (cal/mol. K)			-41.9270	-41.5070	-48.2020	-48.8360
<i>G</i> (au)	-585.8609	-5186.3171	-5772.1494	-5772.1327	-5772.2339	-5772.2163
ΔG (Kcal/mol)			17.9650	28.4055	-35.0426	-23.9972
ν (cm ⁻¹)			-267.4229	-223.3928		

Table 4. Thermodynamic energies of the reaction between α -cis-himachalene and two equivalents of dibromocarbene calculated using DFT B3LYP/6-311+G**

	P ₁ (α)	Dibromo-carbene	TS ₃	TS ₄	P ₂ (α)	P ₂ (β)
<i>E</i> (au)	-5772.5528	-5186.2921	-10958.8386	-10958.8345	-10958.9323	-10958.9237
ΔE (Kcal/mol)			3.9529	6.5358	-54.7898	-49.4296
<i>H</i> (au)	-5772.1680	-5186.2843	-10958.4449	-10958.4405	-10958.5348	-10958.5262
ΔH (Kcal/mol)			4.6254	7.3927	-51.8110	-46.4056
<i>S</i> (cal/mol.K)	138.5690	69.0900	166.9170	164.9630	159.8410	159.9640
ΔS (cal/mol. K)			-40.7420	-42.6960	-47.8180	-47.6950
<i>G</i> (au)	-5772.2339	-5186.3171	-10958.5242	-10958.5189	-10958.6108	-10958.6022
ΔG (Kcal/mol)			16.7727	20.1230	-37.5539	-32.1850
ν (cm ⁻¹)			-279.6469	-301.6563		

1.2.3. Structural analysis of the transition states of the reaction

Analysis of the geometries of the transition states associated with the reaction between α -cis-himachalene and dibromocarbene (Figure 7) shows that the lengths of the bonds formed by chemoisomer 1 are 2.1974 Å at d_1 (C-C₂) and 2.2032 Å at d_2 (C-C₃) for TS₁, and 2.1619 Å at d_1 (C-C₂) and 2.1149 Å at d_2 (C-C₃) for TS₂, while those formed by chemoisomer 2 are 2.2189 Å at d_1 (C-C₇) and 2.1748 Å at d_2 (C-C₁₃) for TS₃ and 2.1781 Å at d_2 (C-C₇) and 2.1939 Å at d_1 (C-C₁₃) for TS₄.

The asynchronicity of bond formation in this reaction can be measured as the difference between the lengths of the two σ bonds formed, namely $\Delta d = d_1 - d_2$. Asynchronicity of chemoisomer 1 is $\Delta d = 0.0877$ Å at TS₁ and $\Delta d = 0.0022$ Å at TS₂, while asynchronicity of chemoisomer 2 is $\Delta d = 0.0123$ Å at TS₃ and $\Delta d = 0.1895$ Å at TS₄. We can conclude that the transition states associated with the two chemoisomeric pathways show that the favoured regioisomers are more asynchronous than the others.

CONCLUSION

The mechanism as well as the chemo-, regio- and stereoselectivity of the reaction between α -cis-himachalene and dibromocarbene was studied using DFT B3LYP/6-311+G**. Analysis of the global electrophilicity and nucleophilicity indices showed that α -cis-himachalene behaves as a nucleophile, while dibromocarbene behaves as an electrophile. The regioselectivity found experimentally was confirmed by local indices of electrophilicity and nucleophilicity, respectively ω_k and N_k .

Calculation of activation energies, analysis of the potential energy surface and IRC calculation shows that this reaction follows a concerted asynchronous mechanism and that whatever quantity of dibromocarbene is used, the favoured electrophile-nucleophile reaction takes place at the α side of the double bond of α -cis-himachalene, leading to the formation of a dibromate product ((1R, 2S, 4R, 7R)-3,3-dibromo-8-methylene-4,12,12-trimethyl-tricyclo[5.5.0.0^{2,4}] dodecane) when the reaction is stoichiometric, and a tetrabromate product ((1R, 2S, 4R, 7R, 8S)-3,3,13,13-tetrabromo-4,12,12-trimethyltricyclo[5.5.0.0^{2,4}]spiro[28]tetradecane) when there is an excess of dibromocarbene.

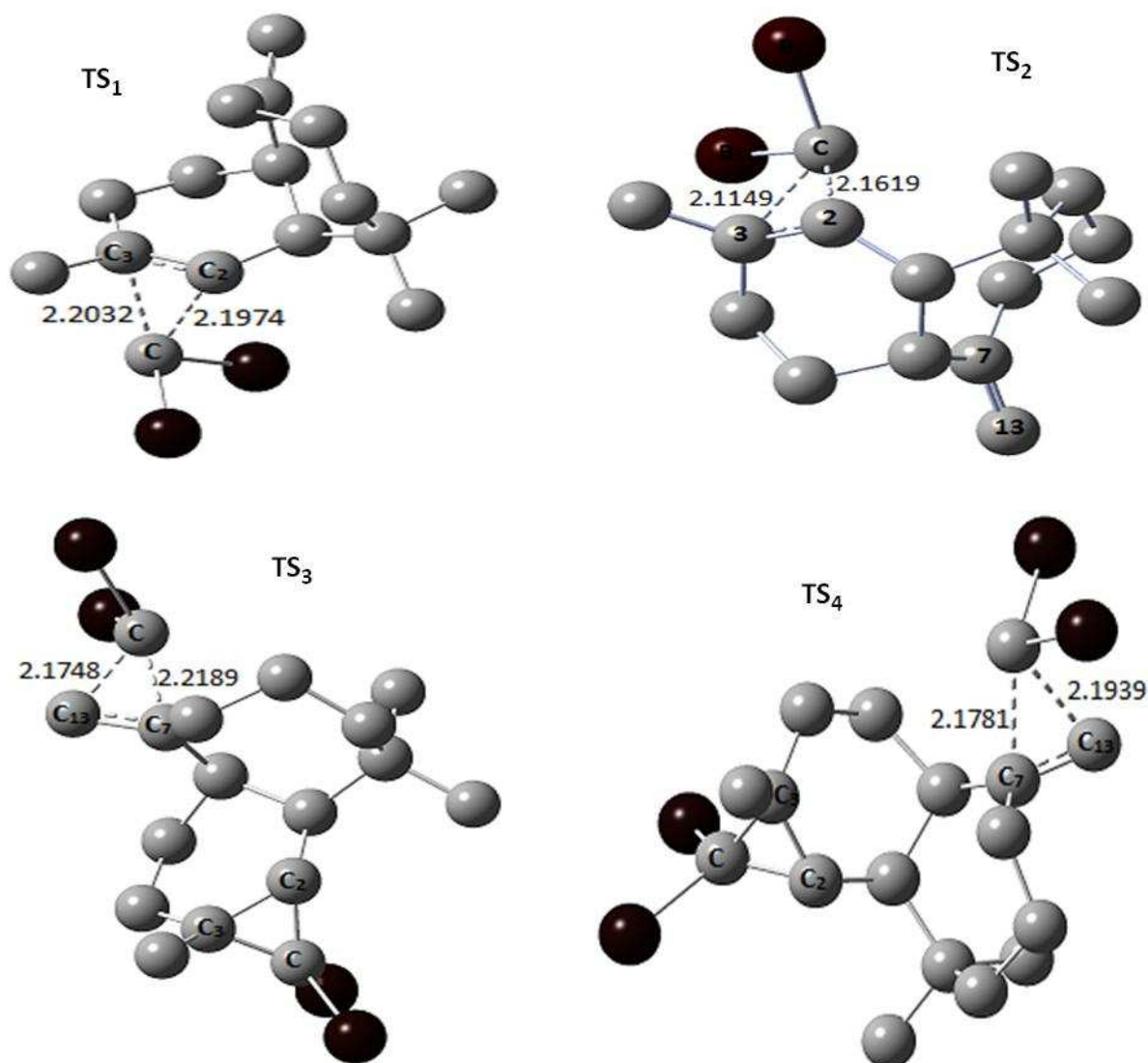


Figure 7. Bond lengths of the transition states of the reaction between α -cis-himachalene and dibromocarbene (Å)

REFERENCES

- [1] R Hammal; A Benharref; A El Hajbi, *Int. J. Inn. App. Stud.*, **2014**, 6, 734-745.
- [2] AS Pfau; P Plattner; *Helv. Chim. Acta*, **1934**, 17, 129-157.
- [3] GS Krishna Rao; Sukh Dev; PC Guha, *Indian Chem. Soc.*, **1952**, 29, 721-730.
- [4] JB Bredenberg; H Erdtmann, *Acta Chem. Scand.*, **1961**, 15, 685-686.
- [5] M Plattier; P Teisseire, *Recherches*, **1974**, 19, 131-144.
- [6] TC Joseph; S Dev, *Tetrahedron*, **1968**, 24, 3809-3827.
- [7] TC Joseph; S Dev, *Tetrahedron*, **1968**, 24, 3841-3852.
- [8] TC Joseph; S Dev, *Tetrahedron*, **1968**, 24, 3853-3859.
- [9] A Benharref; A Bernardini; R Jacquier; PJ Viallefont, *Chem. Research*, **1981**, S, 372-373.
- [10] SC Bisarya; S Dev, *Tetrahedron*, **1968**, 3869-3879.
- [11] R Shankaranyan; S Khrishnappa; S Dev, *Tetrahedron*, **1977**, 3, 885-886.
- [12] M Plattier; Rouillier, P.; Teisseire, P. *Recherches* **1974**, 19, 145-151.
- [13] A Benharref; A Bernardini; R Jacquier; PJ Viallefont, *Chem. Research*, **1981**, 4329-4356.
- [14] A Benharref; A Chekroun; JP Lavergne, *J. P. Soc. Chim. Fr.*, **1991**, 128, 738-741.
- [15] E Lassaba; E Jamili; A Chekroun; A Benharref; A Chiaroni; C Riche; JP Lavergne, *Synth. Commun.*, **1998**, 28, 2641-2651.
- [16] C Lee; W Yang; RG Parr, *Phys. Rev. B*, **1988**, 37, 785-789.
- [17] AD Becke, *J. Chem. Phys.*, **1993**, 98, 5648-5652.
- [18] HB Schlegel. In: *Modern Electronic Structure Theory*, ed. DR Yarkony, World Scientific Publishing, Singapore, **1995**; pp. 459-500.

- [19] KB Wiberg, *Tetrahedron*, **1968**, 24, 1083-1096.
- [20] AE Reed; RB Weinstock; F Weinhold, *J. Chem. Phys.*, **1985**, 83, 735-746.
- [21] AE Reed; LA Curtiss; F Weinhold, *Chem. Rev.*, **1988**, 88, 899-926
- [22] Gaussian 09 (2009) MJ Frisch; GW Trucks; HB Schlegel; GE Scuseria; MA Robb; JR Cheeseman; G Scalmani; V Barone; B Mennucci; GA Petersson; H Nakatsuji; M Caricato; X Li; HP Hratchian; AF Izmaylov; J Bloino; G Zheng; JL Sonnenberg; M Hada; M Ehara; K Toyota; R Fukuda; J Hasegawa; M Ishida; T Nakajima; Y Honda; O Kitao; H Nakai; T Vreven; JA Montgomery Jr; JE Peralta; F Ogliaro; M Bearpark; JJ Heyd; E Brothers; KN Kudin; VN Staroverov; R Kobayashi; J Normand; K Raghavachari; A Rendell; JC Burant; SS Iyengar; J Tomasi; M Cossi; N Rega; NJ Millam; M Klene; JE Knox; JB Cross; V Bakken; C Adamo; J Jaramillo; R Gomperts; RE Stratmann; O Yazyev; AJ Austin; R Cammi; C Pomelli; JW Ochterski; RL Martin; K Morokuma; VG Zakrzewski; GA Voth; P Salvador; JJ Dannenberg; S Dapprich; AD Daniels; Ö Farkas; JB Foresman; JV Ortiz; J Cioslowski; DJ Fox; Gaussian, Inc., Wallingford CT
- [23] RG Parr; W Yang, *Density Functional Theory of Atoms and Molecules*. Oxford University Press, New York, **1989**.
- [24] RG Parr; RG Pearson, *J. Am. Chem. Soc.*, **1983**, 105, 7512-7516.
- [25] P Pérez; LR Domingo; M Duque-Noreña; E Chamorro, *J. Mol. Struct. (Theochem)*, **2009**, 895, 86-91.
- [26] LR Domingo; E Chamorro; P Pérez, *J. Org. Chem.*, **2008**, 73, 4615-4624.
- [27] LR Domingo; MJ Aurell; P Pérez; R Contreras, *J. Phys. Chem. A*, **2002**, 106, 6871-6875.
- [28] LR Domingo; P Pérez; JA Saez, *RSC Advances*, **2013**, 3, 1486-1494.
- [29] P Geerlings; F De Proft; W Langenaeker, *Chem. Rev.*, **2003**, 103, 1793-1873.
- [30] PK Chattaraj; U Sarkar; DR Roy, *Chem. Rev.*, **2006**, 106, 2065-2091.
- [31] LR Domingo; MT Picher; P Arroyo; JA Saez, *J. Org. Chem.*, **2006**, 71, 9319-9330.